Protein Science (1996), 5:2552–2565. Cambridge University Press. Printed in the USA.

NMR studies of structure, hydrogen exchange, and main-chain dynamics in a disrupted-core mutant of thioredoxin

ROBERT DE LORIMIER,[1,2] HOMME W. HELLINGA,[1] AND LEONARD D. SPICER[1,2]

[1]Department of Biochemistry, Duke University Medical Center, Durham, North Carolina 27710
[2]Department of Radiology, Duke University Medical Center, Durham, North Carolina 27710

(RECEIVED July 10, 1996; ACCEPTED September 4, 1996)

Abstract

Core-packing mutants of proteins often approach molten globule states, and hence may have attributes of folding intermediates. We have studied a core-packing mutant of thioredoxin, L78K, in which a leucine residue is substituted by lysine, using ^{15}N heteronuclear two- and three-dimensional NMR. Chemical shift differences between the mutant and wild-type main-chain resonances reveal that structural changes caused by the mutation are localized within 12 Å of the altered side chain. The majority of resonances are unchanged, as are many ^{1}H-^{1}H NOEs indicative of the main-chain fold, suggesting that the structure of L78K is largely similar to wild type. Hydrogen exchange studies reveal that residues comprising the central β-sheet of both mutant and wild-type proteins constitute a local unfolding unit, but with the unfolding/folding equilibrium approximately 12 times larger in L78K. The dynamics of main-chain NH bonds in L78K were studied by ^{15}N spin relaxation and compared with a previous study of wild type. Order parameters for angular motion of NH bonds in the mutant are on average lower than in wild type, suggesting greater spatial freedom on a rapid time scale, but may also be related to different rotational correlation times in the two proteins. There is also evidence of greater conformational exchange in the mutant. Differences between mutant and wild type in hydrogen exchange and main-chain dynamics are not confined to the vicinity of the mutation. We infer that mispacking of the protein core in one location affects local dynamics and stability throughout.

Keywords: dynamics; hydrogen exchange; hydrophobic core; NMR; spin relaxation; structure; thioredoxin

Packing interactions in the hydrophobic core of a protein are an important determinant of its structure and stability (Richards, 1977). A number of combined genetic and biophysical studies have built a consensus view of the response of proteins to mutations in their hydrophobic core (reviewed in Richards & Lim, 1994). In general, it is found that the response to a mutation is remarkably localized, so that proteins can be thought of as plastic materials. The limits of such a plastic response can be tested by introducing highly disruptive mutations in the core, such as charged side chains. Structural and thermodynamic studies of two cases have been presented in the literature. A lysine was introduced (V66K) in the hydrophobic core of staphylococcal nuclease. This mutant is almost as stable as wild type at high pH, but only marginally stable at low pH. Burial of this residue is apparently achieved by significantly lowering the pK_a of the amino group. The X-ray structure of this mutant (Stites et al., 1991) was determined under conditions where the lysine was deprotonated (pH 8.8), and showed that the lysine was located in a completely nonpolar environment in the apparent absence of any obvious electrostatic stabilization or formation of salt bridges or hydrogen bonds. The crystal structure of a T4 lysozyme mutant (M102K), where K102 is buried in the hydrophobic core, shows that the mutant structure is similar to wild type (WT), indicating a plastic response (Dao-pin et al., 1991). Even though the mean structure had not changed, crystallographic *B*-factors of the substituted position and a few residues nearby had increased significantly, indicating that the region surrounding the mutant lysine had become more mobile. This suggested a model in which the deleterious burial of lysine is accommodated by the equilibrium between two states. In one state, the lysine is buried; in the other, the helix covering it is disordered to some degree, allowing solvation of the charged ε-amino group.

Reprint requests to: Leonard D. Spicer, Department of Biochemistry, Box 3711, Duke University Medical Center, Durham, North Carolina 27710; e-mail: spicer@trublu.biochem.duke.edu.

Abbreviations: L78K, thioredoxin with Leu 78 substituted by Lys; WT, wild type; DQ-COSY, double-quantum filtered correlation-spectroscopy; TOCSY, total correlation spectroscopy; NOESY, NOE spectroscopy; HSQC, heteronuclear single-quantum coherence; $\Delta\delta$, difference in chemical shift; PF, protection factor for hydrogen exchange; T_1, longitudinal relaxation time; T_2, transverse relaxation time; S^2, order parameter; τ_m, molecular correlation time; τ_e, effective internal correlation time; R_{ex}, exchange factor for relaxation; $J(\omega)$, value of the spectral density function at frequency ω.

Position 78 in the hydrophobic core of *Escherichia coli* thioredoxin is unusual in that the WT leucine can be replaced with all possible charged amino acids (Hellinga et al., 1992). Differential scanning calorimetry of lysine- and arginine-substituted mutants L78K and L78R showed that in addition to the mutants having reduced stability, their folded states showed a significant increase in heat capacity (Ladbury et al., 1995), indicating that changes in solvent exposure must have occurred. The mutant L78R also binds analinonaphthalenesulfonic acid, unlike L78K and WT, which suggests it approaches a compact intermediate folding state. Neither mutant protein has yet been crystallized.

We are studying the dominant structure, local stability, and local dynamics in these thioredoxin mutants as models of the states that precede final folding of a closely packed native protein. In the current study of packing mutant L78K, solution NMR has been used to assess (1) structural differences with WT from chemical shift values and NOEs indicative of global fold, (2) local structural stability by measuring hydrogen exchange rates, and (3) local dynamics from nuclear spin-relaxation rates. For these purposes, ^{15}N-enriched L78K and WT protein were produced to facilitate detection of individual amide NH resonances. ^{15}N is also a nucleus suited to relatively simple modeling of spin-relaxation in terms of molecular motion.

Chemical shift is a function of the environment of a nucleus and an indicator of changes in molecular structure. Local differences in structure between L78K and WT were assessed by comparison of ^{15}N, NH, and C$^{\alpha}$H chemical shifts in the two proteins, and of ^{1}H-^{1}H NOEs indicative of the main-chain fold. Structural stability in localized regions of L78K and WT was evaluated by measuring the exchange rate of hydrogen between solvent water and individual amide groups. These rates were interpreted in terms of the local-unfolding model (Englander & Mayne, 1992), in which it is assumed that protein structure can be disrupted temporarily in localized regions, leading to breakage of intramolecular hydrogen bonds as a minimal requirement for amide hydrogen exchange. Examination of exchange data for various residues in thioredoxin identifies potential unfolding units or quasi-stable substructures. A comparison of exchange data between L78K and WT reveals details of changes in local stability resulting from amino acid substitution.

Descriptions of motion in the peptide backbone of L78K at individual amides were derived from measurements of three parameters associated with ^{15}N spin-relaxation: T_1, T_2, and {^{1}H}-^{15}N NOE. The main variable governing such relaxation is the radial motion of the N-H bond vector. The probability of such motion occurring at a particular frequency is given by the spectral density function. The values of this function at five discrete frequencies can be determined if sufficient ^{15}N single-spin and ^{15}N-^{1}H two-spin relaxation rates are measured (Peng & Wagner, 1992a, 1992b). If only single-spin rates are known, then estimates of spectral density values at three frequencies can be obtained (Farrow et al., 1995; Ishima & Nagayama, 1995), as described below in a comparison of spectral density values in L78K and WT. Information about motions can also be obtained by modeling the spectral density function in terms of two separate motions: overall molecular tumbling and the independent rapid motions of individual NH groups (Lipari & Szabo, 1982). Values for parameters describing these motions are derived by fitting the modeled spectral density function to spin-relaxation rates. The results of applying such an analysis to L78K are presented below in comparison with the previous analysis of WT thioredoxin (Stone et al., 1993).

The relation between NH bond dynamics and properties of molecular structure is examined. Spectral density values and modeled spectral density parameters for individual amide NH, as well as differences between the two proteins in these quantities, are compared with structural characteristics such as distance from the site of side-chain substitution, number of main-chain hydrogen bonds, differences in chemical shift, proximity to the molecular surface, and secondary structure. The results are discussed in terms of a model in which disruption of packing in L78K leads to changes in structure and to dynamic adaptation.

Results

Main-chain assignment and structural implications

Resonance assignments for the main-chain nuclei NH, ^{15}N, and C$^{\alpha}$H, of thioredoxin L78K, as well as most side-chain hydrogens, were determined from homo- and heteronuclear two-dimensional (2D) and three-dimensional (3D) correlation and NOESY spectra. A substantial similarity between the spectra of L78K and WT obtained in this work, together with the published WT assignment (Dyson et al., 1989; Chandrasekhar et al., 1991), facilitated the assignment of L78K. Resonances were not assigned for NH and ^{15}N of Ser 1, Asp 2, and Gly 33; ^{15}N for any of the five prolines; and C$^{\alpha}$H of Ser 1. In the assignment of WT, it was found that the main-chain ^{15}N and NH of Asp 2 and Gly 33 were difficult to detect, presumably due to rapid hydrogen exchange (Dyson et al., 1989). A list of the main-chain assignments for L78K is available in the Electronic Appendix. Resonance assignments for ^{15}N and NH of WT thioredoxin were derived from the HSQC spectrum by direct comparison to published values obtained under slightly different buffer conditions (Chandrasekhar et al., 1991). Values of C$^{\alpha}$H chemical shift for WT under these conditions were determined from DQ-COSY, 2D NOESY, and ^{15}N-edited HSQC-NOESY spectra.

Chemical shift is sensitive to the environment of a nucleus, allowing structural differences between two similar proteins to be detected without a full 3D structure determination. Differences in ^{15}N, NH, and C$^{\alpha}$H chemical shift ($\Delta\delta$) of L78K relative to WT thioredoxin were calculated for each residue, and are presented in Figure 1. It is seen that chemical shift differences are low for most residues, but are large for several, in particular residues 26–28, 35–39, 41–43, 56–58, 77–79, and 90–95, all of which are within 12 Å of position 78 (Figs. 1B, 2). Nuclei more distant than 12 Å from C$^{\beta}$ of Leu 78 show almost no difference in chemical shift. The greatest differences occur in residues 90–95, comprising residues of strand β5 that are adjacent to the mutated portion of β4, and the loop connecting β5 to α4, which circumscribes the side chain of residue 78 (Fig. 2). Other particularly affected regions are residues 25–28 in β2 adjacent to the mutated segment of β4, and residues 35, 38, and 41 of helix α2, the side chains of which approach that of Leu 78 in WT thioredoxin. In general, residues on the side of the β-sheet where the side chain of residue 78 protrudes show larger differences in chemical shift than those on the opposite side. The lack of large chemical shift differences overall is evidence that the structure of L78K is not grossly different from WT.

Further evidence for structural similarity between WT and L78K is derived from measurements of NOEs indicative of the global fold of the peptide chain. For example, inter- and intrastrand NOEs between main-chain hydrogens in the β-sheet were measured for both WT and L78K. Of 69 such NOEs observed in oxidized WT

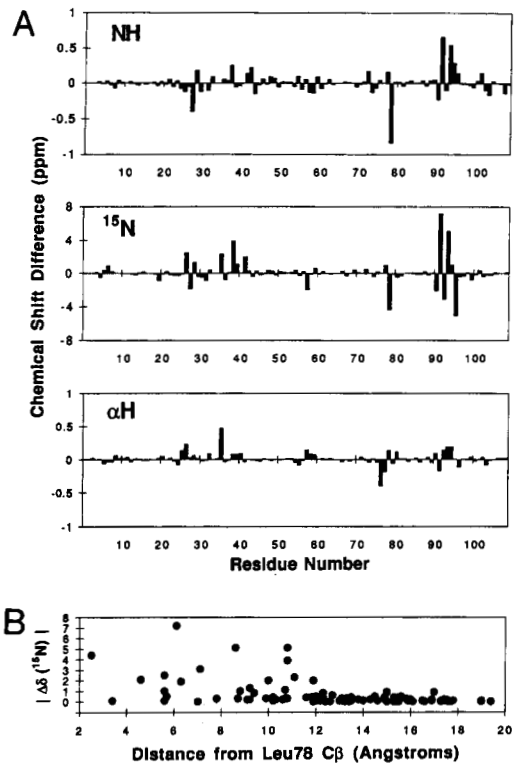

Fig. 1. Chemical shift differences between L78K and WT thioredoxin in main-chain nuclei. **A:** Differences in NH, ^{15}N, and αH chemical shift ($\delta_{L78K} - \delta_{WT}$). **B:** Absolute value of ^{15}N chemical shift difference (ppm) versus distance from C^{β} of Leu 78 in the crystal structure of WT (Katti et al., 1990).

thioredoxin by Dyson et al. (1989), 47 were resolved sufficiently in spectra of both WT and L78K in the current study to allow accurate intensity measurements for comparison. One of these NOEs, that between Lys 90 $C^{\alpha}H$ and Val 91 NH, was unambiguously absent in L78K, but moderately intense in WT. For Val 91 in L78K, the NH correlation peak in HSQC spectra is weak, ^{15}N T_2 is short (see below), and ^{15}N $\Delta\delta$ is large. Thus, the failure to detect an NOE between Lys 90 $C^{\alpha}H$ and Val 91 NH in L78K could be due to differences with WT in structure and/or chemical exchange. The other 46 NOEs were present in each protein. The ratio of volumes, NOE_{L78K}/NOE_{WT}, was derived for each of the 46 well-resolved β-sheet NOEs. The mean value of the ratio, normalized to 1.0 because of differences in the NOESY spectra due to sample concentration and line shape, had a standard deviation of 0.68, a lower limit of 0.09 (Val 55 $C^{\alpha}H$–Leu 24 NH), and an upper limit of 3.7 (Trp 28 $C^{\alpha}H$–Ala 29 NH). The variation in this ratio about the mean may be due to three factors: (1) error in volume measurement, (2) differences between WT and L78K in internal dynamics, and (3) differences in structure. The error in NOE volume due to measurement reproducibility and background noise is estimated to be approximately 10%, giving a standard deviation of 0.14 in the ratio of NOEs. Thus, other factors, such as differences in dynamics and structure, contribute considerably to differences in interproton NOE intensity in L78K and WT. In the absence of detailed structural and dynamics information, quantitation of L78K NOEs in terms of a relaxation matrix is not feasible. Assuming simply that each NOE arises from an isolated pair of ^{1}H nuclei, the various NOE ratios may be translated into ratios of distance, because NOE depends on the inverse sixth power of distance. Using this assumption, the normalized mean ratio for interproton distances in the β-sheet of WT and L78K is 1.0, with a standard deviation of 0.10, and upper and lower limits of 1.35 and 0.85, respectively. Approximately 80% of interproton distances in the β-sheet of L78K are within 10% of the WT distance, according to this simplified model. Because the contributions of dynamics and relaxation by neighboring hydrogens to NOE have been ignored, the actual deviation in interproton distance is likely to be less.

Hydrogen exchange in main-chain amides

Amide hydrogen exchange rates were measured in WT and L78K thioredoxin by rapidly changing the solvent from H_2O to D_2O, then acquiring ^{15}N-edited HSQC spectra to measure NH signal intensity as a function of time. The intensity of each NH signal was fit to a single exponential, yielding a pseudo-first-order rate constant, k_{ex} (h^{-1}). Under the conditions of the experiment, most of

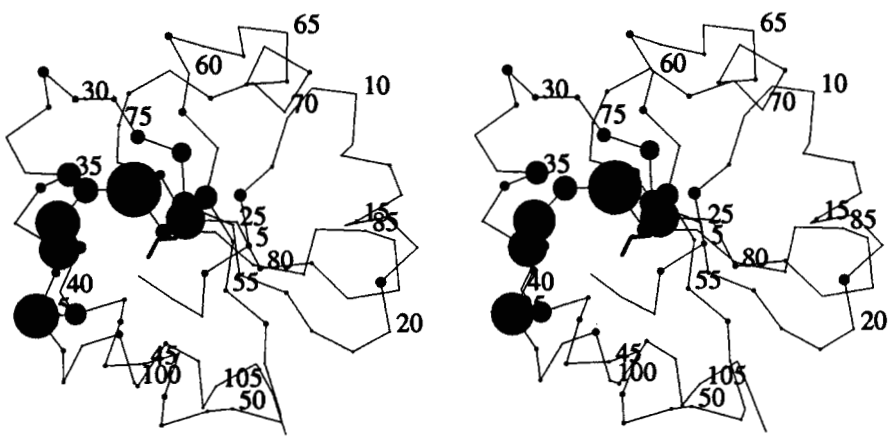

Fig. 2. Stereo view of the trace of main-chain nitrogen atoms in WT thioredoxin. Nitrogen atoms are shown as circles with diameters proportional to the absolute value of the difference in chemical shift of ^{15}N between WT and L78K. The largest radius (Val 91) has $|\Delta\delta| = 7.2$ ppm. The side-chain bonds of Leu 78 are shown as thicker rods. Note that most of the large shifts are located in the loop that covers position 78. Atomic coordinates are those of molecule A in the crystal structure (Katti et al., 1990).

the amide NH signals fell below the limit of noise by the first postexchange HSQC spectrum. These rapidly exchanging amides ($k_{ex} > 3\ h^{-1}$) all occur near the protein surface in WT thioredoxin, and many do not participate in intramolecular hydrogen bonds.

In WT thioredoxin, 39 amides had signal intensity above background in at least the first three spectra, permitting derivation of a rate constant for each (Table 1). For L78K, k_{ex} was obtained for 38 amides, all of which were also measured in WT. The NH not measured in L78K was Leu 42, which was undetectable in the first time point, and hence $k_{ex} > 3\ h^{-1}$. The rate constant given for Cys 35 in L78K could have a contribution from Ile 75 because the two residues have coincident amide ^{15}N and H chemical shifts. It is assumed that Ile 75 of L78K, as in WT, is highly exposed on the protein surface and exchanges too rapidly to measure. The decay of this signal did not require a double exponential to be fit adequately. A more complete determination of amide hydrogen exchange rates in oxidized WT thioredoxin has been reported recently (Jeng & Dyson, 1995). The solution conditions of that study differ from the present one, but a comparison of data from the two shows that relative exchange rates for individual amides are very similar.

Other than Leu 42, there were eight residues for which the NH cross peak in one of the two proteins had decayed beyond detec-

Table 1. *Hydrogen exchange rates and protection factors of main-chain amides in WT and L78K thioredoxin*

	k_{ex} (h^{-1})		Protection factor ($\times 10^{-6}$)			
Residue	WT	L78K	WT	L78K	WT/L78K	Population[a]
Ile 5	8.1	3.3	0.00027	0.00066	0.41	f
Thr 8	1.6	2.1	0.0067	0.0051	1.3	f
Val 16	1.1	2.0	0.0023	0.0013	1.8	f
Leu 17	0.26	0.44	0.015	0.0087	1.7	f
Ile 23	0.00095	0.0064	3.9	0.58	6.7	s
Leu 24	0.0011	0.0073	2.8	0.42	6.7	s
Val 25	0.00083	0.0038	2.9	0.65	4.5	s
Asp 26	0.00067	0.012	11	0.61	18	s
Phe 27	0.26	0.49	0.029	0.016	1.8	f
Trp 28	0.0012	0.013	7.6	0.68	11	s
Ala 29	0.0074	0.047	2.1	0.33	6.4	s
Cys 35	1.1	2.7	0.043	0.017	2.5	f
Leu 42	0.19	>3	0.016	<0.00096	>16	f
Glu 44	3.2	3.1	0.0013	0.0013	1.0	f
Ile 45	0.096	0.14	0.012	0.0081	1.5	f
Ala 46	0.13	0.17	0.088	0.071	1.2	f
Thr 54	0.046	0.048	0.23	0.22	1.1	f
Val 55	1.3	1.4	0.005	0.0046	1.1	f
Ala 56	0.0012	0.023	12	0.64	19	s
Lys 57	0.17	0.084	0.11	0.22	0.50	f
Leu 58	0.00092	0.021	7.5	0.32	23	s
Ile 60	0.0026	0.024	2.9	0.32	9.1	s
Asp 61	0.46	2.1	0.013	0.0028	4.6	f
Asn 63	1.9	2.5	0.050	0.039	1.3	f
Ala 67	3.3	4.3	0.0096	0.0072	1.3	f
Tyr 70	1.5	1.3	0.0094	0.011	0.85	f
L78, K78	0.15	2.0	0.055	0.014	3.9	f
Leu 79	0.00087	0.02	3.7	0.35	11	s
Leu 80	0.0011	0.013	2.9	0.24	12	s
Phe 81	0.00063	0.017	11	0.41	27	s
Lys 82	0.16	0.29	0.13	0.071	1.8	f
Glu 85	0.72	0.44	0.013	0.021	0.62	f
Ala 87	2.7	2.4	0.0053	0.0061	0.87	f
Ala 88	6.9	2.0	0.0029	0.0099	0.29	f
Lys 100	1.3	0.61	0.0084	0.018	0.47	f
Glu 101	0.47	0.15	0.017	0.053	0.32	f
Leu 103	0.0036	0.015	1.7	0.40	4.3	s
Asp 104	0.071	0.061	0.086	0.10	0.86	f
Asn 106	7.5	6.5	0.0082	0.0094	0.87	f
Mean:						
Fast pop.[b]	1.8	1.6	0.038	0.037	1.0	
Slow pop.	0.0018	0.017	5.5	0.46	12	

[a] f, fast population; s, slow population.
[b] Not including Leu 42.

tion by the first HSQC spectrum, but which did not disappear until the second or third spectrum for the other protein. The latter detected NH groups (residues K18, D43, L94 in WT; L7, D47, E48, F102, A105 in L78K) are mostly in helices and all are near the solvent-accessible surface. The data suggest that their NH exchange rates are different in the two proteins. The chemical shift differences of these residues are small (except Leu 94), hence their differential hydrogen exchange rates may be due less to differences in structure than stability. For example, the amide resonances of Phe 102 and Ala 105 in helix α4 are not detectable in the first post-exchange spectrum of WT, but are detected in L78K. Likewise, other amides of helix α4, Lys 100, Glu 101, Asp 104, and Asn 106 all exchange slightly more slowly in L78K than in WT (Table 1). Hence, portions of this helix may be slightly more stable in the mutant.

Figure 3A illustrates the distribution of k_{ex} values in WT and L78K for the 38 residues measured in both proteins. Two populations of amides can be differentiated based on three parameters: exchange rate, width of the distribution in exchange rate, and ratio of exchange rate in the two proteins. The two populations, termed fast and slow, are denoted in Figure 3A by different symbols. The rapidly and slowly exchanging populations have mean k_{ex} of 1.8 h^{-1} and 1.8 $\times$ 10^{-3} h^{-1}, respectively, in WT; and 1.6 h^{-1} and 1.7 $\times$ 10^{-2} h^{-1}, respectively, in L78K. In both proteins, the slow population has a narrower range of exchange rates, and this population in L78K exchanges on average 12 times faster than in WT, as seen by the off-diagonal cluster of points in Figure 3A. In contrast, amides of the fast population exhibit little change in exchange rate between the two proteins, as seen by their clustering along the diagonal in Figure 3A.

In the local-unfolding model for hydrogen exchange (Englander & Mayne, 1992), the equilibrium constant for local structural unfolding is given by k_{ex}/k_{rc} = 1/PF, where k_{rc} is the rate of exchange of the amide in the random coil state, and PF, the protection factor, represents the exchange rate of a protein amide normalized relative to its random coil rate, uninfluenced by secondary structure. The value of k_{rc} for each of the observed 39 residues was calculated according to Bai et al. (1993), then used to derive protection factors, as listed in Table 1. The distribution of PF, illustrated in Figure 3B, shows the same overall pattern as k_{ex} values, i.e., two populations in both WT and L78K, differentiated by the magnitude of PF, width of the distribution in PF, and ratio of PF in the two proteins. Residues comprising the high and low PF populations are the same as those in the slow and fast, respectively, k_{ex} populations. The locations of fast and slowly exchanging amide groups of WT thioredoxin, as well as the free energy of local unfolding derived from PF values ($\Delta G = -RT \ln(1/PF)$) are illustrated in Figure 4A. The 26 residues comprising the fast set (Table 1) consist of hydrogen bonded amides within helices, within turns, and between β-strands at the periphery of the five-stranded β-sheet. The 13 residues of the slow set (Table 1) are almost exclusively located in the central three strands of the β-sheet; the exception being Leu 103, the NH of which forms a hydrogen bond to the carbonyl of Leu 99 in helix α4, and is adjacent to the β-sheet. Differences in the free energy of local unfolding between L78K and WT ($\Delta\Delta G = \Delta G_{L78K} - \Delta G_{WT}$) are illustrated in Figure 4B. The greatest differences are confined largely to amides of the central β-sheet in the hydrophobic core of the protein. Residue Leu 42 is exceptional in that the magnitude of its $\Delta\Delta G$ is large even though it is not in the slowly exchanging population. We hypothesize that the large difference in exchange rate between L78K and WT for Leu 42 is not due solely to a change in local structural stability, but more likely to a change in structure in this region of helix α2. In WT, the amide of Leu 42 is hydrogen bonded to the carbonyl of Ile 38, but large differences in main-chain chemical shifts of Ile 38 suggest that the structure of L78K is altered in the vicinity of this residue. Such changes could increase the exposure of Leu 42 NH to solvent, accelerating its exchange rate in the folded state. In WT, the amide exchange rate of Leu 42 is considerably larger in the reduced state than in the oxidized state, but this was attributed to a change in stability of the active site region rather than differences in structure at Leu 42 (Jeng & Dyson, 1995).

The results of hydrogen exchange measurements are interpreted in light of the local-unfolding model as follows. Amides of the low PF population exchange by numerous and independent local unfolding events, and hence display a broad distribution of PF. Amides of the high PF population exchange in common by a single unfolding event, and thus have a narrow range of PF. The fact that the latter amides are all located in the hydrophobic core of the protein, with most in the center of the β-sheet, suggests that the unfolding event leading to their exchange is global unfolding of the protein structure.

^{15}N spin relaxation studies

Relaxation parameters

Of the 108 residues in L78K, relaxation data were obtained for all but ten main-chain nitrogens. Five of the ten are proline (residues 34, 40, 64, 68, and 76), hence undetectable by the pulse

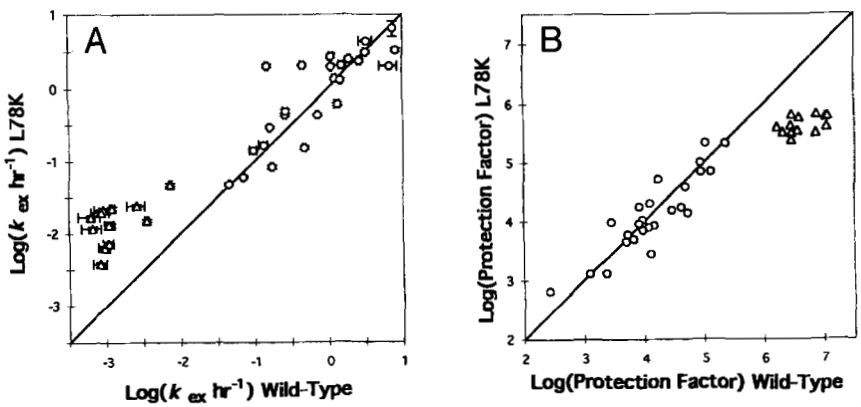

Fig. 3. Hydrogen exchange rates and protection factors of main-chain amides in WT and L78K thioredoxin, indicating two distinct populations. **A:** Logarithm of k_{ex} (h^{-1}) with standard error (shown as bars) for each of 38 residues measured in both proteins. Circles and triangles indicate two populations of amides with differing hydrogen exchange patterns, as discussed in the text. The diagonal line represents equal hydrogen exchange rates in the two proteins. **B:** Logarithm of the protection factor is plotted for each of the 38 amides shown in A. Circles and triangles correspond to the same two populations shown in A. The diagonal line represents equal protection factors in the two proteins.

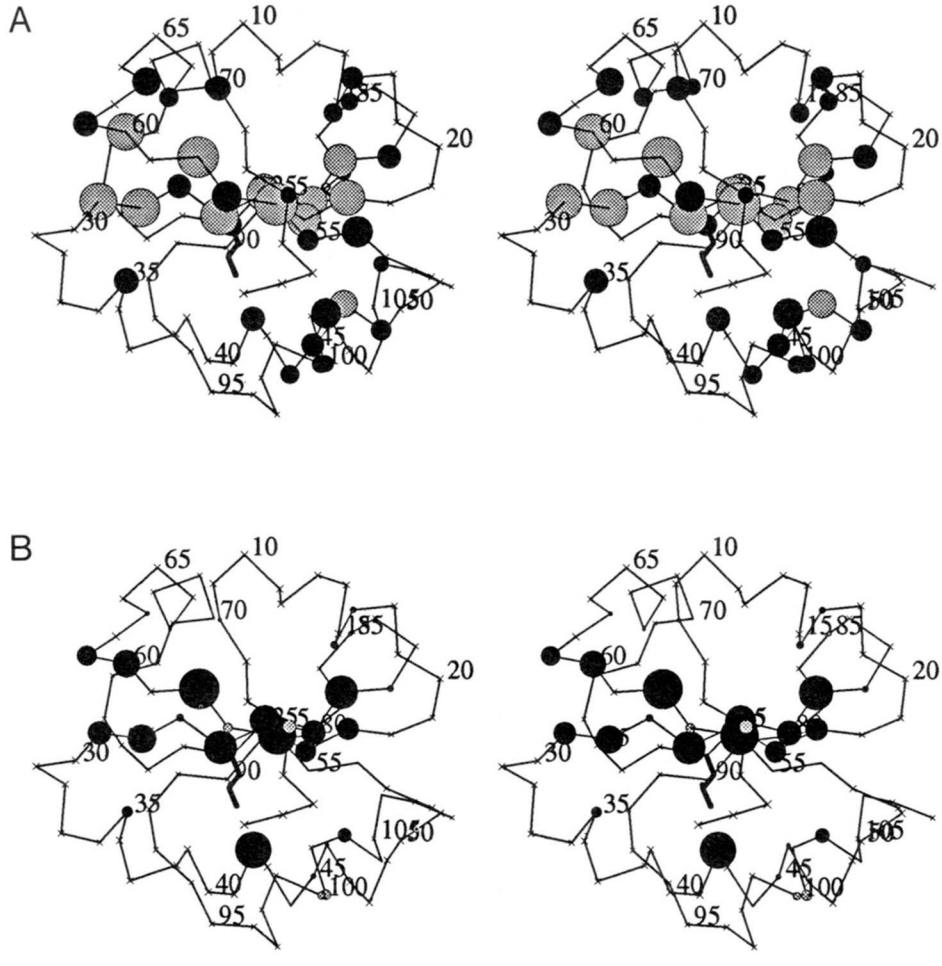

Fig. 4. Free energy of local structural unfolding, derived from amide hydrogen exchange rates, within the 3D structure of WT thioredoxin (Katti et al., 1990). **A:** Amides of WT, for which hydrogen exchange rates were measured, are depicted as circles. The radius of a circle is proportional to the magnitude of the free energy for local unfolding ($\Delta G = -RT \ln(1/PF)$, where PF is from Table 1). The largest radius (Ala 56) is equivalent to $\Delta G = -9.9$ kcal/mol. Solid and shaded circles represent the fast and slow amide-exchange populations, respectively. Small crosses show amides that exchanged too rapidly to measure. **B:** Differences between L78K and WT in the free energy for local unfolding [$\Delta\Delta G = (\Delta G_{L78K} - \Delta G_{WT}) = -RT \ln(PF_{WT}/PF_{L78K})$, where PF is from Table 1]. Solid and shaded circles represent negative and positive $\Delta\Delta G$, respectively. The largest radius (Phe 81) represents $\Delta\Delta G = -2.0$ kcal/mol. The radius of Leu 42 is a lower limit ($\Delta\Delta G = -1.7$ kcal/mol).

schemes used; three residues (Ser 1, Asp 2, and Gly 33) are undetectable because the amide protons apparently exchange rapidly with solvent; and two resonances (Cys 35 and Ile 75) are coincident. The remaining 98 resonances were well resolved and of sufficient intensity to permit measurement of ^{15}N relaxation by indirect detection (Kay et al., 1989; Farrow et al., 1994).

Relaxation times T_1 and T_2, and proton-irradiated ^{15}N NOE values for main-chain ^{15}N (listed in the Electronic Appendix) are graphed in Figure 5, along with the values for WT-oxidized thioredoxin determined by Stone et al. (1993). All three relaxation parameters for main-chain amides in L78K are generally higher than in WT, averaging 19% higher for T_1, 10% for T_2, and 7% for NOE. These parameters depend in part on field strength and correlation time. The static field used in the present studies is higher than that used for WT (17.1 versus 14.7 Tesla; Stone et al., 1993), which would lead to increased T_1 and NOE, but slightly decreased T_2 for L78K assuming equal correlation times for the two proteins. The fact that higher T_2 values are observed for L78K suggests the possibility that its correlation time is actually lower than WT, as is borne out by modeling and analysis of the spectral density function (see below). A difference in correlation time is also suggested from measurement of ^1H linewidths in one-dimensional (1D) spectra. For example, the well resolved methyl resonances of Val 16 each have a linewidth of 13.5 Hz in L78K and 17.4 Hz in WT. Because linewidth is approximately proportional to rotational correlation time, the latter value for WT is apparently about 29% greater than L78K under the solution conditions of the experiment. It should be noted that exchange processes such as internal conformation or multimerization may also contribute to differences in relaxation rate and linewidths.

A residue-by-residue comparison of relative relaxation parameters (Fig. 5) shows qualitatively that amide bond dynamics are largely similar in the two proteins. For example, in both proteins, T_1 and T_2 values of residues 3, 4, 21, 22, 74, 94, and 108 are higher than average, whereas the ^{15}N NOE is lower, suggesting a greater contribution from high-frequency motions for these amide bond vectors.

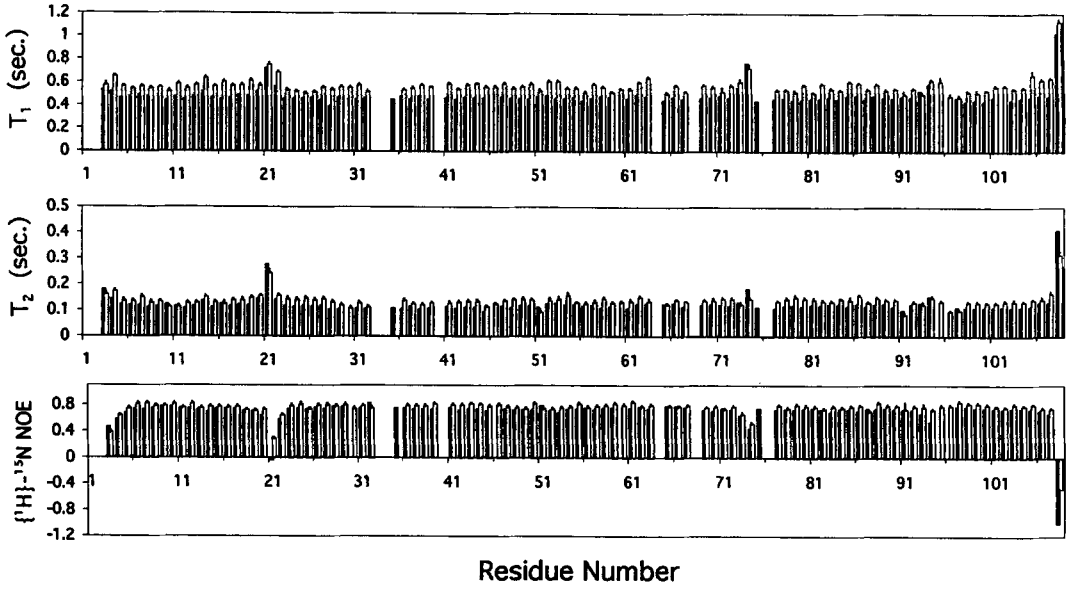

Fig. 5. Comparison of main-chain ^{15}N spin-relaxation parameters, T_1, T_2, and $\{^1H\}$-^{15}N NOE, in L78K and WT thioredoxin. Values for L78K are shown as open bars, each with an appended segment denoting the standard error. Values for WT (Stone et al., 1993) are shown as closed bars, with errors omitted.

Spectral density modeling

The Lipari and Szabo (1982) spectral density parameters τ_m, S^2, and τ_e, and the exchange term R_{ex} (Clore et al., 1990), were derived from the 98 residues of L78K for which relaxation data were obtained (listed in the Electronic Appendix). A unique value of τ_m was fit, based on the nearly spherical dimensions of oxidized WT thioredoxin (Stone et al., 1993). The value obtained, 5.42 ± 0.02 ns, is significantly lower than the 6.41 ± 0.04 ns obtained for WT. Such a discrepancy most likely reflects differences in molecular properties. Calorimetric measurements of protein unfolding in WT (Ladbury et al., 1993) and L78K (Ladbury et al., 1995) suggest an equilibrium between monomer and dimer in both proteins, with a greater tendency of WT to dimerize. Applying the modeled equilibrium constant for dimerization of WT (Ladbury et al., 1993) under the solution conditions at which ^{15}N relaxation studies were performed (Stone et al., 1993), the protein is estimated to be 44 mole percent in the form of dimer. In the present study L78K is estimated to be less than 4 mole percent dimer. Hence, the higher τ_m value for WT likely reflects an average for the population of monomer and dimer. In comparing WT and L78K in terms of ^{15}N relaxation rates and parameters derived from them, dissimilar aggregation states of the two proteins must be considered. A less likely source of discrepancy in τ_m values is differences between the pulse sequences used to measure spin relaxation for the current study (Farrow et al., 1994) and for WT (Stone et al., 1993). The differences are minor and expected to affect the sensitivity of measurement rather than observed magnetization decay rates.

Numerically derived values of the order parameter S^2 in L78K and WT (Stone et al., 1993) are plotted versus amino acid sequence in Figure 6. The error in S^2 for L78K, indicated in Figure 6, is estimated by Monte-Carlo simulation to be generally less than 2%. S^2 values in the two proteins vary similarly along the amino acid chain. For example, S^2 in residues 3, 4, 21, 74, 75, 94, and 108 are lower than average in both proteins. These residues generally occur in loops or at the ends of regular secondary structures. Residues in the L78K sequence near the position of mutation do not show atypical deviations in S^2. A general pattern is that S^2 values in L78K are lower than in WT; in fact, the mean S^2 of L78K (0.81 ± 0.09) is significantly lower than for WT (0.86 ± 0.11) in the 91 residues for which values were obtained for both proteins (one-tailed t-test, $p < 0.01$). This observation suggests that, on average, fast angular motion of NH bond vectors in L78K is slightly less restricted than in WT.

The parameter τ_e is related to both the rate and amplitude of internal motion faster than τ_m, and thus is not readily interpretable in the absence of a defined model of motion. Figure 6 shows τ_e in L78K and WT (Stone et al., 1993). Except for the ten residues of L78K that were not measured, the absence of a bar indicates that the fit value of τ_e was zero. It must be noted that τ_e is highly sensitive to small variations in relaxation parameters and hence its error from Monte-Carlo simulation is large, averaging approximately 40%. In general values of τ_e for residues in WT exceed those of L78K. Large differences in τ_e between L78K and WT are seen at several positions. In particular, τ_e for residues 36–42 is consistently higher in WT. This segment is in the middle of helix $\alpha 2$ and contains several residues, such as Met 37 and Ile 38, which also have large chemical shift differences.

The exchange term, R_{ex}, applied in fitting spectral density parameters to T_2 (Clore et al., 1990), is also plotted in Figure 6. Like τ_e, this term has a relatively high error for most residues, averaging approximately 30%. Except for the ten unmeasured residues of L78K, the absence of a bar in the figure signifies that R_{ex} was estimated to be zero. It was estimated to be greater than zero for 41 residues in L78K, 23 of which coincide with WT residues having non-zero values of R_{ex} (Stone et al., 1993). The mean value of R_{ex} is higher in L78K (1.14 s^{-1}) than WT (0.70 s^{-1}) for residues in which this parameter was non-zero. For instance, there are 12 residues where R_{ex} is at least 1.0 s^{-1} greater in L78K than in WT, but only two residues where WT R_{ex} is at least 1.0 s^{-1} higher than L78K. Residues that differ by more than 1 s^{-1} in R_{ex} between the

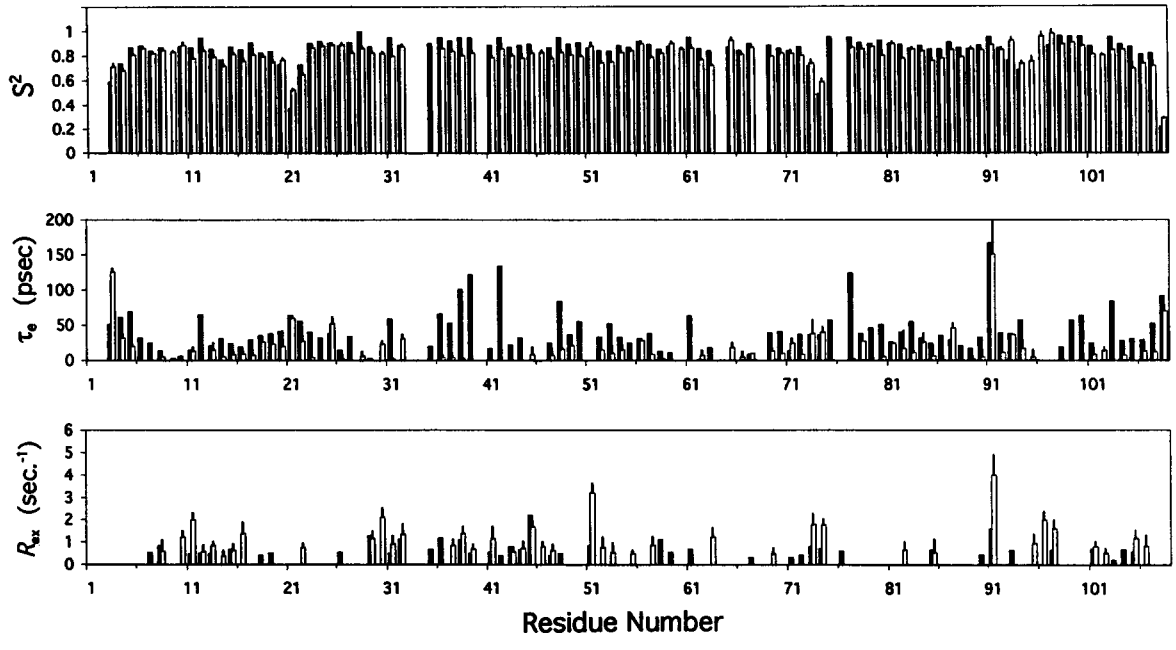

Fig. 6. Comparison of modeled spectral density parameters S^2, τ_e, and R_{ex} for main-chain amides in L78K and WT thioredoxin. Values for L78K are shown as open bars, each with an appended segment denoting the standard error. Values for WT (Stone et al., 1993) are shown as closed bars, with errors omitted. The error in τ_e for Val 91 of L78K is ±570 ps.

two proteins are found throughout the structure of WT thioredoxin, but one, Val 91, is near the site of mutation, with its amide N 6.1 Å from Leu 78 C^{β}. Hence, main-chain amides in L78K appear to exhibit more rapid conformational exchange than in WT.

Quasi-spectral density mapping

The value of the spectral density function, $J(\omega)$, for a given amide bond vector can be mapped directly for five frequencies from ^{15}N single-spin and ^{1}H-^{15}N two-spin relaxation rates (Peng & Wagner, 1992a). In the absence of two-spin rates, values of the spectral density can be estimated at three frequencies (zero, ω_N, and $\omega_H + \omega_N$) by approximating $J(\omega_H - \omega_N) \sim J(\omega_H) \sim J(\omega_H + \omega_N)$ (Farrow et al., 1995; Ishima & Nagayama, 1995). Estimated values $J(0)$, $J(\omega_N)$, and $J(\omega_H + \omega_N)$ in L78K, where $\omega_N = -3.82 \times 10^8$ rad/s and $\omega_H + \omega_N = 3.39 \times 10^9$ rad/s, were determined from ^{15}N T_1, T_2, and $\{^1H\}$-^{15}N NOE. The results are plotted in Figure 7, along with values for WT derived by Ishima and Nagayama (1995) from the relaxation data of Stone et al. (1993). It must be noted that, in the case of WT, $\omega_N = -3.17 \times 10^8$ and $(\omega_N + \omega_H) = 2.81 \times 10^9$ rad/s due to the different static fields at which relaxation was measured. Hence, a direct comparison of L78K and WT in terms of $J(\omega_N)$ and $J(\omega_N + \omega_H)$ is not strictly valid, but a comparison of relative values is. Values of $J(0)$ in the two proteins are directly comparable.

From Figure 7, it is seen that amides of L78K having relatively low values of $J(0)$ and $J(\omega_N)$ often have high values of $J(\omega_H + \omega_N)$. Examples are amides of residues 3, 4, 21, 22, 73, 74, and 108. This indicates that the spectral density function for such amide NH is more broadly distributed than most; that is, the motions are shifted toward higher frequencies (Peng & Wagner, 1992b). These same residues also have the lowest S^2 values from spectral density

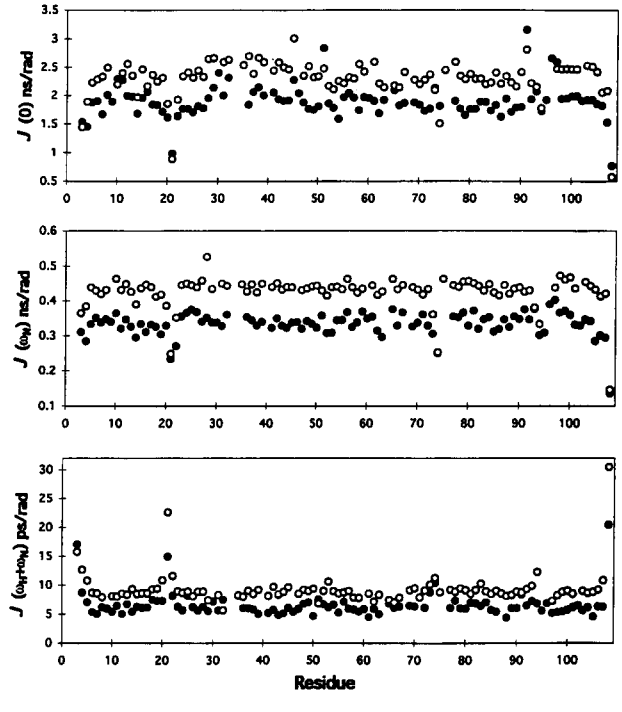

Fig. 7. Quasi-spectral density values for main-chain amides at three frequencies in L78K and WT thioredoxin. Filled and open circles represent L78K and WT, respectively. For L78K $\omega_N = -3.8 \times 10^8$ rad/s, and $\omega_H + \omega_N = 3.4 \times 10^9$ rad/s. For WT $\omega_N = -3.2 \times 10^8$ rad/s, and $\omega_H + \omega_N = 2.8 \times 10^9$ rad/s. Quasi-spectral density values for WT were derived previously by Ishima and Nagayama (1995). The average coefficient of error for residue-specific spectral density values in L78K are $J(0)$, 4%; $J(\omega_N)$, 2%; $J(\omega_H + \omega_N)$, 8%.

modeling, indicating greater freedom of motion on a time scale faster than τ_m. On the other hand, residues 30, 51, 91, 96, and 97 of L78K have the highest $J(0)$ values, yet do not have $J(\omega_H + \omega_N)$ values that are unusually low. This suggests that, rather than having a relatively narrow distribution of motion, their calculated $J(0)$, which is greatly dependent on T_2, is artificially high due to a significant contribution of exchange line-broadening to T_2. Supporting this interpretation is the observation that these residues have the highest R_{ex} values in the spectral density modeling analysis (see Fig. 6). Thus, these amides likely undergo conformational exchange.

In comparing L78K to WT in terms of quasi-spectral density analysis, it is seen that the trend in $J(\omega)$ values with sequence in both proteins is largely similar (Fig. 7). For example, residues 3, 4, 21, 22, 74, 75, and 108 in both proteins have relatively low $J(0)$ and $J(\omega_N)$, and high $J(\omega_H + \omega_N)$. Some significant exceptions are noted. Residues 51, 96, and 97 have atypically high $J(0)$ values in L78K but not in WT. As discussed above, high $J(0)$ values in the absence of unusually low $J(\omega_H + \omega_N)$ values may indicate conformational exchange, hence suggesting motional differences in the two proteins for residues 51, 96, and 97.

As pointed out by Peng and Wagner (1992b), the characteristic correlation time of an individual motion, τ_R, is related to $J(0)$ as follows: $J(0) = 2/5\ \tau_R$, and the overall molecular correlation time is approximated by the upper limit of τ_R for all residues. Thus, the difference in molecular correlation time between L78K and WT can, in principle, be estimated from the differences in their maximal $J(0)$. However, the higher values of $J(0)$ may include contributions from exchange and lead to inaccurate estimates of τ_R. A potentially less biased estimate of the difference in molecular correlation time may be determined from the difference in mean τ_R for all amide N. The mean τ_R for amide N in L78K obtained from the mean of $J(0)$ is 4.70 ns, and for WT is 5.72 ns. Thus, quasi-spectral density analysis corroborates spectral density modeling in demonstrating a correlation time for L78K that is 1.0-ns shorter than WT.

There appear to be differences between the values of $J(0)$ for L78K and WT that cannot be ascribed simply to differing molecular correlation time. If the two molecules differed only in tumbling rate, then the difference in $J(0)$ [$\Delta J(0) = J(0)_{L78K} - J(0)_{WT}$] evaluated over all amides would be a distribution having a mean equal to the difference in molecular correlation time and a variance equal to that expected from propagation of the error in $J(0)$ for individual amides. The F statistic was used to test the hypothesis that the variance of the distribution of $\Delta J(0)$ over all 91 amides is equal to the variance expected from the contribution of measurement error to individual $J(0)$ values. The hypothesis was rejected ($p < 0.01$) and, in fact, the variance of $\Delta J(0)$ is greater than expected from measurement error alone. Thus, the distribution of $\Delta J(0)$ is not that of the same protein at two different tumbling rates. Two explanations are: (1) that residue-specific dynamics differences occur between the two proteins, as suggested by differences in S^2; or (2) that partial aggregation of WT accounts for the differences in $J(0)$ in ways other than simply increasing the molecular tumbling rate.

Dynamics and structure

The structural basis for NH bond dynamics is unknown, hence the possibility of links between dynamics and various parameters of structure was examined. The five structural parameters considered were: (1) distance from the solvent-accessible surface; (2) chemical-shift difference between L78K and WT; (3) distance from the site of side-chain substitution; (4) category of secondary structure; and (5) number of main-chain hydrogen bonds to the amide group.

Distance from the solvent-accessible surface. A structural parameter that appears correlated with dynamics is proximity to the molecular surface. The surface was defined according to the method of Connolly (1983) by a probe solvent of 1.4-Å radius, in contact with WT oxidized thioredoxin (Katti et al., 1990), including hydrogen atoms. The shortest distance from each main-chain nitrogen to the surface was then calculated, and is referred to as its depth. The values of $J(0)$, S^2, and their respective differences (L78K − WT) are plotted in Figures 8 and 9 as a function of amide N depth.

The behavior of $J(0)$ with depth in both proteins is shown in the scatter plots of Figure 8A and B. In each case, values of $J(0)$ vary greatly near the surface. However, general trends in $J(0)$ with depth are revealed by plotting the moving average of $J(0)$ in order of depth (Fig. 8D,E). In the case of WT, a trend of increasing $J(0)$ with depth is apparent. This suggests that motions near the surface of WT tend to have higher frequencies, indicative of more motion independent of molecular tumbling than found in the interior. In the case of L78K, such a trend is lacking or much smaller. The value of $\Delta J(0)$, a measure of differences in dynamics between L78K and WT, shows an obvious trend with depth, (Fig. 8C,F) being minimal (closer to zero) near the surface, and tending toward a maximal absolute deviation in the interior. Hence, on average surface residues in the two proteins are more similar in dynamics than those interior.

The value of $\Delta J(0)$ for interior residues is expected to correspond closely to the difference in molecular correlation time, because angular motion in these amides is presumed to be largely dependent on rotational diffusion of the molecule (Peng & Wagner, 1992b). In the present case, $\Delta J(0)$ values for the ten deepest residues (24, 25, 26, 27, 28, 42, 56, 78, 79, and 80) have a mean of -0.59 (± 0.11) ns/rad, which corresponds to a difference in molecular correlation time of -1.48 (± 0.28) ns. However, a difference of -1.0 (± 0.04) ns was suggested by the two different estimates presented above. This discrepancy suggests that core amides in L78K have correlation times that are lower than expected from a simple difference with WT in molecular correlation time. Hence, the mutation may have caused a shift toward higher frequency motions for interior amides of L78K.

The order parameter S^2 also exhibits a depth dependence in both proteins (Fig. 9), ranging from a minimum of approximately 0.75 near the surface to a maximum of 0.92 (WT) or 0.85 (L78K) for the deepest amides (Fig. 9D,E). This might be expected because surface amides presumably have fewer restraints on their motions than interior amides. The value of ΔS^2 is also dependent on depth. Because S^2 is modeled to be independent of τ_m (Lipari & Szabo, 1982), no trend in ΔS^2 with depth is expected if motional restrictions for NH bond vectors are unchanged in the two proteins. The fact that ΔS^2 is minimal (approaching zero) at the surface is consistent with the idea that these amides move relatively independently of the protein as a whole, as evidenced by their low $J(0)$ values. On the other hand, the magnitude of ΔS^2 is greatest toward the interior, suggesting that core amides in L78K are less restricted on average than in WT in their motions.

Chemical shift difference. To test for a correlation between structural perturbation and changes in dynamics, chemical shift differences ($\Delta\delta$ for ^{15}N, NH, and $C^{\alpha}H$) were plotted separately versus

differences in relaxation rates (ΔT_1, ΔT_2, ΔNOE), spectral density parameters (ΔS^2, $\Delta \tau_e$, ΔR_{ex}), and spectral density at zero frequency [$\Delta J(0)$]. No overall correlation was apparent; that is, residues having large differences in chemical shift do not usually exhibit large deviations in dynamic properties (not shown). Only three residues, Val 91, Ala 93, and Leu 94, have large deviations in chemical shift as well as in relaxation rates, spectral density parameters, and $J(0)$. Thus, in these cases, the amino acid substitution at position 78 has affected both structure and dynamics.

Distance from the site of side-chain substitution. The possibility of a link between differences in dynamics and distance from the site of amino acid substitution was also examined. The difference between the two proteins in relaxation rates, S^2, R_{ex}, and $J(0)$ for each amide nitrogen, was plotted versus its distance from Leu 78 C^β, as measured from the crystal structure of oxidized WT (Katti et al., 1990). No correlation is apparent in such plots (not shown), or when a moving average of the respective quantity is plotted versus distance (in terms of incremental order) from Leu 78 C^β, suggesting that differences between L78K and WT in NH bond dynamics are not confined to the vicinity of the mutation.

Category of secondary structure. Main-chain amides were categorized into β-strands, helices, reverse turns, or irregular structures following the secondary structure assignment of Katti et al. (1990). For each category, the average value of S^2, $J(0)$, and their respective differences between the two proteins were calculated (tabulated in the Electronic Appendix). The order parameter S^2 shows a relation with secondary structure in that the mean S^2 for irregular structures is significantly lower than for turns, β-strands, and helices. Secondary structure is also correlated with $\Delta S^2 = (S^2_{L78K} - S^2_{WT})$, because the mean value of ΔS^2 for amides in irregular structures is significantly less negative (approximately zero) than in other categories, suggesting that motions in irregular structures are not greatly altered by the mutation. Values of $J(0)$ vary with secondary structure in a manner similar to S^2. For ex-

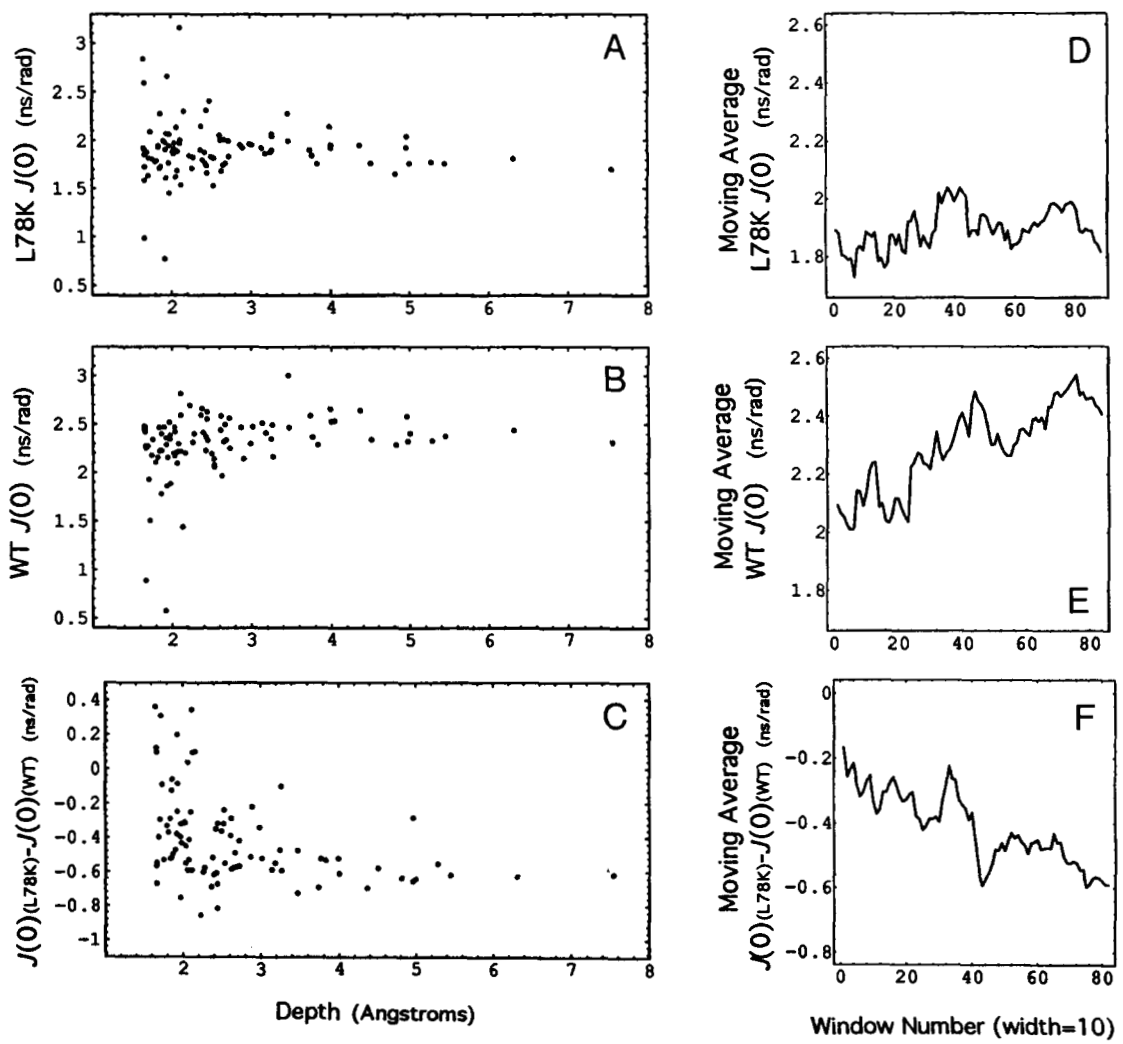

Fig. 8. Quasi-spectral density values at zero frequency [$J(0)$] for main-chain amides as a function of minimum distance from the solvent-accessible surface (depth). Depth is calculated from the crystal structure of WT thioredoxin (Katti et al., 1990) using a solvent-accessible surface generated by the Connolly (1983) algorithm. **A,B:** $J(0)$ values in L78K and WT thioredoxin, respectively, as a function of depth. **C:** Residue-specific difference in $J(0)$ between L78K and WT as a function of depth. **D,E:** Average $J(0)$ in L78K and WT, respectively, in windows of ten residues stepped sequentially from the shortest to greatest depth. **F:** Average residue-specific difference of $J(0)$ in windows of ten residues stepped sequentially from shortest to greatest depth.

ample, irregular structures have significantly lower values of $J(0)$ than other classes of secondary structure, and irregular structures show the least difference between L78K and WT.

Number of main-chain hydrogen bonds. Each ^{15}N was categorized as to whether its amide group has zero, one, or two hydrogen bonds to other backbone amides (Katti et al., 1990). For amide groups with one hydrogen bond, a distinction was not made as to whether the hydrogen bond occurred through the CO or NH moiety. Average values of S^2, ΔS^2, $J(0)$, and $\Delta J(0)$ for each category were determined (tabulated in the Electronic Appendix). For each of these parameters, a significant difference (one-tailed t-test, $p < 0.05$) between each hydrogen bond category was found in terms of the mean value of the particular parameter. For each protein, values of $J(0)$ and S^2 progressively increase with zero, one, or two hydrogen bonds per amide. The single exception is $J(0)$ in L78K, where no difference is found between one and two hydrogen bonds. Values of ΔS^2 and $\Delta J(0)$ decrease progressively with zero, one, or two hydrogen bonds. Thus, the number of hydrogen bonds to main-chain amide groups is correlated with amide N dynamics. The amide group as a whole, including the CO moiety, appears to act as a dynamic unit, because no differences were found between single hydrogen bonds at the NH or CO (not shown).

Discussion

The results of this study reveal changes in structure, structural stability, and main-chain dynamics resulting from replacement of an amino acid side chain contributing to the hydrophobic core of a protein. The substitution has not prevented the attainment of an overall native-like structure; the evidence suggests that the greatest changes are localized to a peripheral loop. However, these structural differences do not coincide with changes in local stability, as inferred from hydrogen exchange rates. In particular, the greatest difference in stability is a uniform increase in L78K of hydrogen exchange rates in the central β-sheet. This sheet acts as a local unfolding unit in both the WT and substituted proteins, but is more stable in the former.

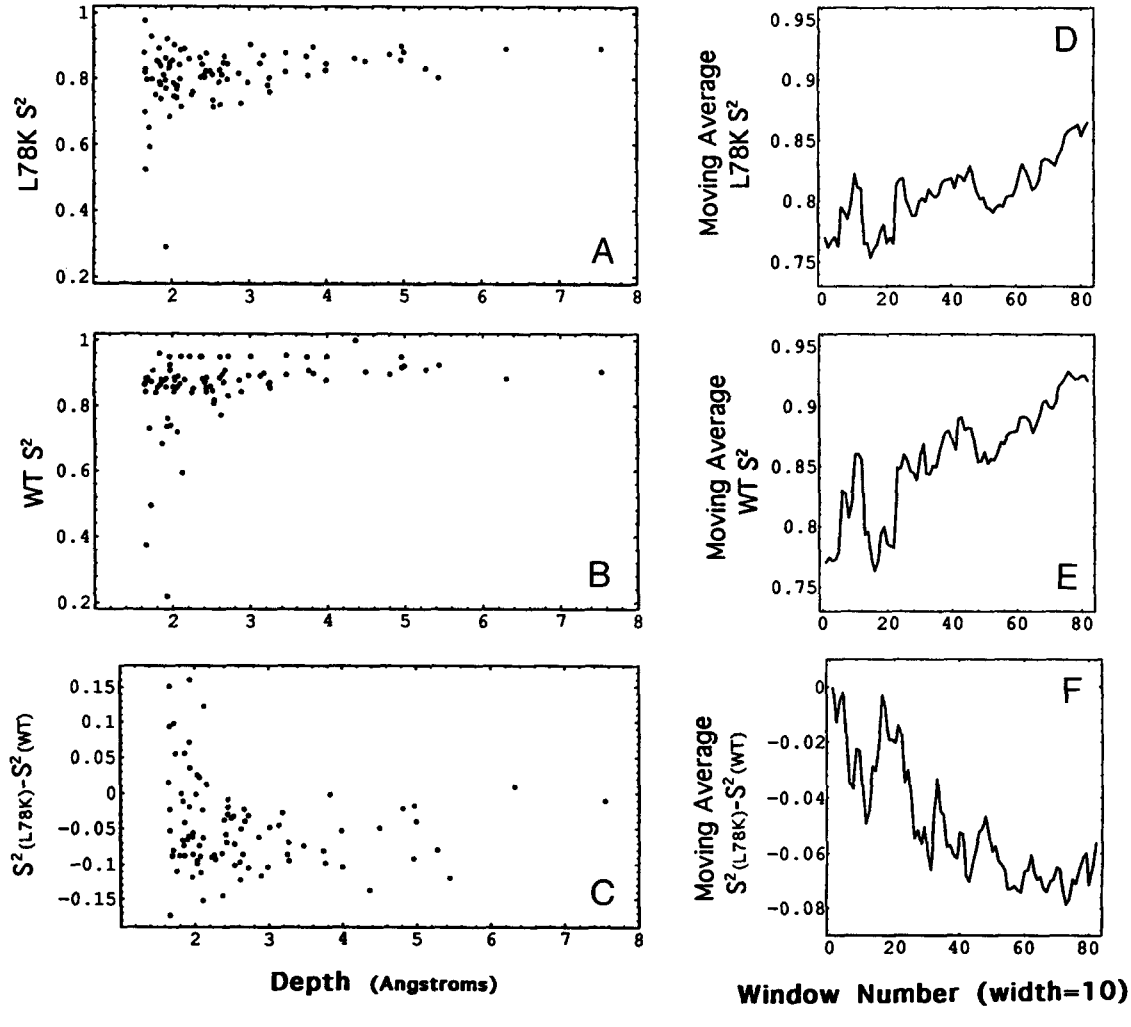

Fig. 9. Order parameters (S^2) for main-chain amides as a function of minimum distance from the solvent-accessible surface (depth). Depth is calculated from the crystal structure of WT thioredoxin (Katti et al., 1990) using a solvent-accessible surface generated by the Connolly (1983) algorithm. **A,B:** S^2 in L78K and WT, respectively, as a function of depth. **C:** Residue-specific difference in S^2 as a function of depth. **D,E:** Average S^2 in L78K and WT, respectively, in windows of ten residues stepped sequentially from the shortest to greatest depth. **F:** Average residue-specific difference of S^2 in windows of ten residues stepped sequentially from the shortest to greatest depth.

Characterization of overall molecular motion from ^{15}N relaxation measurements revealed a molecular correlation time for L78K of 5.4 ns, which is 1.0 ns less than that determined for WT (Stone et al., 1993). This difference may be due to the greater tendency of WT to aggregate, possibly as a dimer (Ladbury et al., 1993), thus yielding a value of τ_m representing the population average. Parameters of main-chain amide dynamics in L78K, derived by modeling the spectral density function and by quasi-spectral density analysis, also showed differences between L78K and WT. The order parameter S^2 is lower on average in L78K than WT, and spectral density values, $J(0)$, in L78K differ from those expected on the basis of differing molecular correlation time. These differences suggest that frequencies for amide motions in L78K are higher than in WT. However, other hypotheses may account for dissimilar dynamics parameters in the two proteins. One alternative is that aggregation in WT causes a shift toward low-frequency amide motions. Another hypothesis is that the modeled order parameter is not independent of overall molecular correlation time. Thus, the higher average values of S^2 in WT may reflect a dependence on τ_m, the value of which is higher in WT than L78K. However, these hypotheses do not appear to hold in at least one case, that of an SH2 domain (Farrow et al., 1994). In comparing dynamics parameters of two forms of SH2 domain, free or complexed with phosphopeptide, the two had substantially different τ_m (9.2 and 6.5 ns, respectively), due to aggregation of the uncomplexed form. Yet, the average S^2 values for main-chain amide NH were identical (0.80) in both forms. Hence, in this case, τ_m and S^2 appear to be independent. If thioredoxin is analogous, then differences in order parameter would be consistent with disruption of core packing.

Differences between WT and L78K in dynamics parameters correlate poorly with distance from the site of mutation or with chemical shift difference, but do correlate with distance from the molecular surface. The greatest differences in parameters describing main-chain motions are found for the most interior residues. Differences in main-chain dynamics are also correlated with the number of main-chain hydrogen bonds, as observed in human ubiquitin (Schneider et al., 1992), and with secondary structure, although these two structural parameters are cross-correlated and also correlated with distance from the molecular surface. Hence, a direct link between NH bond dynamics and any single structural parameter is not demonstrated.

L78K may be regarded as a model of an intermediate state in the folding of thioredoxin. It does not resemble a molten globule state (Ptitsyn, 1992), as do some core mutants in other proteins (Lim et al., 1992), although the mutant of thioredoxin in which arginine is substituted for Leu 78 may approximate such a state (Ladbury et al., 1995). L78K is functional in vivo and fairly stably folded, but appears from thermodynamic (Ladbury et al., 1995) and denaturation (Hellinga et al., 1992) studies to be closer energetically to an unfolded state than is WT. Furthermore, main-chain amides throughout L78K, but especially those interior, exhibit higher mobility than in WT. Several residues in L78K also show evidence, in terms of R_{ex} and $J(0)$, of greater conformational exchange. Hence, a protein that is nearly completely folded, except for mispacking in one region, has main-chain dynamics that may be considered more fluid than in the optimally packed state.

It is clear that proteins can employ several distinct mechanisms to accommodate mutations in the hydrophobic core. Mutations in which steric packing effects predominate, such as change in size without change in polarity, appear to be accommodated primarily by a static, plastic structural response (Richards & Lim, 1994). Introduction of a charged group in the core creates a situation in which, in addition to packing considerations, the constraints of the hydrophobic effect are perturbed severely. In all cases where such a deleterious mutation can be accommodated, the stability of the native state is diminished significantly by the mutation. The question is how this free energy is redistributed between the states that the mutant can adopt. In one case, the pK_a of a buried lysine is perturbed to such an extent that the ϵ-amino group is uncharged, and the buried lysine behaves as a hydrophobic residue (Stites et al., 1991). This can also be thought of as a static structural adaptation. However, in the case of the M102K mutant in T4 lysozyme (Dao-pin et al., 1991) and, in particular, in the case presented in this work, it is clear that there may also be a significant dynamic response.

Materials and methods

Protein purification

WT and L78K mutant thioredoxin were expressed from plasmids pHH30 and pHH121, respectively, (Hellinga et al., 1992) in *E. coli* strain DH5α. Cells were grown in defined mineral medium containing glucose and supplemented with nucleoside bases and vitamins. Nitrogen was supplied as [^{15}N]-NH_4Cl (97% isotopic purity, Cambridge Isotope Laboratories) at 1.0 g/L. Thioredoxin expression was induced with 1 mM isopropyl-β-D-galactoside when cultures reached an optical density of 0.8–1.0 (600 nm). Purification of WT and L78K thioredoxins followed a previous protocol (Hellinga et al., 1992) except that the following step was introduced prior to gel filtration. Protein precipitated by 75%-saturated $(NH_4)_2SO_4$ was dissolved in 20 mM Tris-HCl, pH 7.4, then solid NaCl was added to 4.0 M. The solution was clarified by centrifugation and loaded on a column of Phenyl-Sepharose CL-4 (Pharmacia). Proteins were eluted with a linear salt gradient from 4.0 M to 0.0 M NaCl, then fractions enriched in thioredoxin were concentrated by ultrafiltration prior to gel filtration. After ion-exchange chromatography, thioredoxin was concentrated and exchanged into NMR buffer by ultrafiltration using a Centricon-10 apparatus (Amicon). The protein solution for all NMR spectroscopy (except hydrogen exchange, see below) was 2.3–2.5 mM thioredoxin, 10% D_2O, 100 mM KH_2PO_4, pH 6.7, 2 mM NaN_3, 1 mM sodium 3-(trimethylsilyl) propionate.

NMR spectroscopy

Spectra were collected on a Varian Unity 600 MHz spectrometer with a triple resonance probe equipped for pulsed-field z-gradients. All spectra were acquired at a temperature of 308 K and employed ^{15}N-decoupling during directly and indirectly acquired ^1H evolution periods.

Resonance assignment

Homonuclear pulse sequences employed were DQ-COSY (Piantini et al., 1982; Rance et al., 1983), TOCSY (Levitt et al., 1982; Bax & Davis, 1985) (80–110-ms mixing time), and NOESY (Jeener et al., 1979) (150-ms mixing time). Water suppression was achieved by selective saturation. Two-dimensional ^{15}N-edited HSQC spectra (Kay et al., 1992) had spectral widths of 9,000 Hz for ^1H and 3,500 Hz for ^{15}N, collected as 1,024 and 512 complex points, respectively. Three-dimensional ^{15}N-edited HSQC-TOCSY and

HSQC-NOESY spectra (Zhang et al., 1994) had HSQC planes of 9,000 Hz for ^1H and 2,200 Hz for ^{15}N, collected as 1,024 and 32 complex points, respectively. The indirectly acquired ^1H dimension was 9,000 Hz with 128 complex points. The mixing time for HSCQ-TOCSY was 64 ms, and for HSQC-NOESY was 150 ms. Heteronuclear pulse sequences all employed pulsed field gradients for coherence selection and used sensitivity enhancement (Palmer et al., 1991).

Relaxation measurements

Pulse sequences used for determining values of ^{15}N T_1, T_2, and $\{^1H\}$-^{15}N NOE were those of Farrow et al. (1994) in which saturation of water was minimized. The spectral widths in each spectrum were 9,000 Hz (^1H) and 3,500 Hz (^{15}N), collected as 1,024 and 256 complex points, respectively. To measure ^{15}N T_1, eight spectra were obtained with T relaxation periods of 32.4, 64.8, 129.6, 270.1, 497.0, 799.5, 1,199.2, and 1,998.7 ms. A delay of 2.0 s followed each acquisition, and two transients were collected per $t1$ increment. To measure ^{15}N T_2, eight spectra were obtained with T relaxation periods of 15.7, 31.5, 63.0, 94.4, 125.9, 188.9, 251.8, and 503.7 ms. The delay between acquisitions was 2.0 s and two transients were collected for each $t1$ increment. $\{^1H\}$-^{15}N NOE was determined from spectra in which transients acquired with and without ^1H saturation were collected in an interleaved fashion. A relaxation delay of 5 s followed each acquisition, and 16 transients were collected per $t1$ increment.

Hydrogen exchange

A spin-column was prepared of Sephadex G-25 equilibrated with 0.10 M KH_2PO_4, 2 mM NaN_3 in a solvent of 99.9% D_2O, having a nominal pH of 6.70 (not corrected for deuterium isotope effect). The Sephadex beads had been pre-exchanged by suspending in 99.9% D_2O and lyophilizing prior to suspension in the D_2O buffer. Thioredoxin solution (0.65 mL) in phosphate-buffered 90% H_2O/10% D_2O was passed through the column (3.0-mL packed volume) by centrifugation at room temperature, then immediately transferred to an NMR sample tube and placed in the spectrometer for temperature equilibration and shimming. Acquisition of the first spectrum was initiated 10 min after the solvent had been exchanged. A total of 16 (WT) or 17 (L78K) ^{15}N-edited HSQC spectra was acquired over 9 (WT) or 7 (L78K) days, at intervals increasing from 10 min initially to 48 h at the end. Spectra had widths of 9,000 Hz (^1H) and 3,500 Hz (^{15}N). The first five were collected as 1,024 × 128 (^1H × ^{15}N) complex points, whereas subsequent spectra had 1,024 × 256 complex points. All were acquired with a single transient per $t1$ increment. For the purpose of normalizing NH cross peak intensity among the spectra, 1D proton spectra were acquired immediately prior to the first, sixth, 13th, and each subsequent HSQC spectrum. In the interval between acquisition of the last three or four time points, the sample was removed from the magnet and stored at 308 K. VNMR software (Varian) was employed for spectral processing. Two-dimensional FIDs were zero-filled to 2,048 points in both dimensions prior to applying gaussian apodization and Fourier transformation. Peak intensities were recorded using the *ll2d* routine of VNMR. One-dimensional spectra were processed by zero-filling to 8,192 points, then performing Fourier transformation without prior apodization. Baselines were corrected with a polynomial function, then areas of individual baseline-resolved NH and $C^\alpha H$ peaks were obtained by integration.

Fitting relaxation rates

For ^{15}N T_1 and T_2 relaxation, the peak intensities at varying relaxation times were fit to the expression $I_t = I_o \exp(-t/T)$, where t is the relaxation delay, I_t is the observed peak intensity at time t, and I_o and T are parameters fit using Quasi-Newton minimization in SYSTAT software (Evanston, Illinois). T is taken as the relaxation time, and the error in T is determined from the covariance matrix of the fit. From NOE spectra, the $\{^1H\}$-^{15}N NOE of a peak was calculated as the ratio of its intensity in the presence of ^1H saturation to that in the absence of saturation. The error in NOE was determined by propagation of the error in peak intensity, which in turn was estimated as the RMS of baseplane noise in the respective spectra (Farrow et al., 1994).

Fitting hydrogen exchange rates

It was necessary to normalize NH peak intensities between sets of HSQC spectra because (1) the first five spectra were acquired with half as many points in the ^{15}N dimension as subsequent spectra, and (2) the last three or four spectra were obtained after removal and re-insertion of the sample over a period of several days, hence causing slight changes in the field due to factors such as sample position and cryogen level. The amide hydrogens of two residues, F81 and V25, were baseline-resolved in 1D spectra, as was the $C^\alpha H$ peak of Leu 78 (WT) or Lys 78 (L78K). For each 1D spectrum, the ratio of the area of each of these two amide peaks to the nonexchangeable $C^\alpha H$ of residue 78 was used to normalize the corresponding NH peak intensities in the 2D spectrum acquired immediately (less than 3 min) afterward. Then the exchange time was derived by fitting normalized peak intensity at each time point to a first-order decay, as described above for ^{15}N relaxation time.

Spectral density modeling

The spectral density function proposed by Lipari and Szabo (1982) contains three parameters: τ_m, the correlation time for overall molecular tumbling, which is unique for a spherical molecule; τ_e, the effective correlation time for motion of a bond vector much faster than τ_m; and S^2, the order parameter (without units) describing the spatial restriction of rapid radial motion. An additional variable, R_{ex} (units of s^{-1}), is also invoked in fitting T_2 relaxation rates (Clore et al., 1990). This parameter accounts for shortening of T_2 due to effects other than transverse relaxation, such as conformational exchange, that have lifetimes longer than τ_m but shorter than the CPMG recycle time (~1 ms). The Lipari and Szabo model has been applied to study NH bond dynamics in WT thioredoxin, both oxidized and reduced (Stone et al., 1993). The method of that analysis was followed exactly in the current study, taking into account a higher field strength (14.1 Tesla), to derive τ_m, τ_e, S^2, and R_{ex}. Errors in spectral density parameters were estimated from 100 Monte-Carlo simulations, as opposed to 500 in the study by Stone et al. (1993). Calculations were performed using Mathematica (Wolfram Research, Inc., Champaign, Illinois) software.

Quasi-spectral density mapping

Estimates of the value of the spectral density function at three frequencies, 0 rad/s, $\omega_N = -3.82 \times 10^8$ rad/s, and $\omega_H + \omega_N = 3.39 \times 10^9$ rad/s, were obtained according to Ishima and Nagayama (1995). They and Farrow et al. (1995) proposed an approximation of the equations relating relaxation times T_1, T_2, and

RN [the heteronuclear cross-relaxation rate, where NOE = 1 + $\gamma_H/\gamma_N(RN)(T_1)$], to spectral density. Specifically, they assume $J(\omega_H + \omega_N) \sim J(\omega_H) \sim J(\omega_H - \omega_N)$, thus allowing the three quantities $J(0)$, $J(\omega_N)$, and $J(\omega_H + \omega_N)$ to be solved directly given the three measured relaxation parameters T_1, T_2, and NOE. Errors in $J(\omega)$ were determined by Monte-Carlo simulations using the errors in relaxation parameters.

Molecular modeling

Molecule A of oxidized WT thioredoxin (Katti et al., 1990) was modeled with InsightII (Biosym, San Diego, California). A dot surface representing solvent-accessible area (Connolly, 1983) was calculated using a probe of 1.4-Å radius touching thioredoxin, including hydrogens, at a dot density of 1-Å^{-2}. A file containing the coordinates of each dot was used to calculate the distance from a given main-chain nitrogen to each dot. The smallest such value was taken as the minimum distance of the nitrogen to the solvent-accessible surface.

Supplementary material in Electronic Appendix

Seven text files are available tabulating (1) main-chain resonance assignments for L78K, (2) amide ^{15}N spin-relaxation parameters for L78K, (3) NH spectral-density parameters for L78K, (4) order parameters for NH in secondary structures of L78K and WT, (5) spectral density values for NH in secondary structures of L78K and WT, (6) order parameter versus main-chain hydrogen bonds in L78K and WT, and (7) spectral density value versus main-chain hydrogen bonds in L78K and WT.

Acknowledgments

These studies were supported in part by NIH grants GM49871 (H.W.H.) and GM41829 (L.D.S.). The Duke NMR Center was established with partial support from the NIH, NSF, and North Carolina Biotechnology Center. We thank Dr. Ronald Venters of the Duke University NMR Center for assistance in acquisition of NMR spectra; and Frederic M. Richards and Richard Wynn for unlabeled mutant protein, stimulating discussions, and encouragement.

References

Bai Y, Milne JS, Mayne L, Englander SW. 1993. Primary structure effects on peptide group hydrogen exchange. *Proteins Struct Funct Genet 17*:75–86.

Bax A, Davis DG. 1985. MLEV-17-based two-dimensional homonuclear magnetization transfer spectroscopy. *J Magn Reson 65*:355–360.

Chandrasekhar K, Krause G, Holmgren A, Dyson HJ. 1991. Assignment of the ^{15}N NMR spectra of reduced and oxidized *Escherichia coli* thioredoxin. *FEBS Lett 284*:178–183.

Clore GM, Driscoll PC, Wingfield PT, Gronenborn AM. 1990. Analysis of the backbone dynamics of interleukin-1β using two-dimensional inverse detected heteronuclear ^{15}N-^1H NMR spectroscopy. *Biochemistry 29*:7387–7401.

Connolly ML. 1983. Solvent-accessible surfaces of proteins and nucleic acids. *Science 221*:709–713.

Dao-pin S, Anderson DE, Baase WA, Dahlquist FW, Matthews BW. 1991. Structural and thermodynamic consequences of burying a charged residue within the hydrophobic core of T4 lysozyme. *Biochemistry 30*:11521–11529.

Dyson HJ, Holmgren A, Wright PE. 1989. Assignment of the proton NMR spectrum of reduced and oxidized thioredoxin: Sequence-specific assignments, secondary structure, and global fold. *Biochemistry 28*:7074–7087.

Englander SW, Mayne L. 1992. Protein folding studied using hydrogen-exchange labeling and two-dimensional NMR. *Annu Rev Biophys Biomol Struct 21*:243–265.

Farrow NA, Muhandiram R, Singer AU, Pascal SM, Kay CM, Gish G, Shoelson SE, Pawson T, Forman-Kay JD, Kay LE. 1994. Backbone dynamics of a free and a phosphopeptide-complexed Src homology 2 domain studied by ^{15}N NMR relaxation. *Biochemistry 33*:5984–6003.

Farrow NA, Zhang O, Szabo A, Torchia DA, Kay LE. 1995. Spectral density-function mapping using ^{15}N relaxation data exclusively. *J Biomol NMR 6*:153–162.

Hellinga HW, Wynn R, Richards FM. 1992. The hydrophobic core of *Escherichia coli* thioredoxin shows a high tolerance to nonconservative single amino acid substitutions. *Biochemistry 31*:11203–11209.

Ishima R, Nagayama K. 1995. Protein backbone dynamics revealed by quasi spectral density function analysis of amide N-15 nuclei. *Biochemistry 34*:3162–3171.

Jeener J, Meier BH, Bachmann P, Ernst RR. 1979. Investigation of exchange processes by two-dimensional NMR spectroscopy. *J Chem Phys 71*:4546–4553.

Jeng MF, Dyson HJ. 1995. Comparison of the hydrogen-exchange behavior of reduced and oxidized *Escherichia coli* thioredoxin. *Biochemistry 34*:611–619.

Katti SK, LeMaster DM, Eklund H. 1990. Crystal structure of thioredoxin from *Escherichia coli* at 1.68 Å resolution. *J Mol Biol 212*:167–184.

Kay LE, Keifer P, Saarinen T. 1992. Pure absorption gradient enhanced heteronuclear single quantum correlation spectroscopy with improved sensitivity. *J Am Chem Soc 114*:10663–10665.

Kay LE, Torchia DA, Bax A. 1989. Backbone dynamics of proteins as studied by ^{15}N inverse detected heteronuclear NMR spectroscopy: Application to staphylococcal nuclease. *Biochemistry 28*:8972–8979.

Ladbury JE, Wynn R, Hellinga HW, Sturtevant JM. 1993. Stability of oxidized *Escherichia coli* thioredoxin and its dependence on protonation of the aspartic acid residue in the 26 position. *Biochemistry 32*:7526–7530.

Ladbury JE, Wynn R, Thomson JA, Sturtevant JM. 1995. Substitution of charged residues into the hydrophobic core of *Escherichia coli* thioredoxin results in a change in heat capacity of the native protein. *Biochemistry 34*:2148–2152.

Levitt MH, Freeman R, Frenkiel T. 1982. Broadband heteronuclear decoupling. *J Magn Reson 47*:328–330.

Lim WA, Farruggio DC, Sauer RT. 1992. Structural and energetic consequences of disruptive mutations in a protein core. *Biochemistry 31*:4324–4333.

Lipari G, Szabo A. 1982. Model-free approach to the interpretation of nuclear magnetic resonance relaxation in macromolecules. 1. Theory and range of validity. *J Am Chem Soc 104*:4546–4559.

Palmer AG III, Rance M, Wright PE. 1991. Intramolecular motions of a zinc finger DNA-binding domain from Xfin characterized by proton-detected natural abundance ^{13}C heteronuclear NMR spectroscopy. *J Am Chem Soc 113*:4371–4380.

Peng JW, Wagner G. 1992a. Mapping spectral density functions using heteronuclear NMR relaxation measurements. *J Magn Reson 98*:308–332.

Peng JW, Wagner G. 1992b. Mapping of the spectral densities of N-H bond motions in eglin c using heteronuclear relaxation experiments. *Biochemistry 31*:8571–8586.

Piantini U, Sorenson OW, Ernst RR. 1982. Multiple quantum filters for elucidating NMR coupling networks. *J Am Chem Soc 104*:6800–6801.

Ptitsyn OB. 1992. The molten globule state. In: Creighton TE, ed, *Protein folding*. New York: WH Freeman. pp 243–300.

Rance M, Sorenson OW, Bodenhausen G, Wagner G, Ernst RR, Wuthrich K. 1983. Improved spectral resolution in COSY ^1H NMR spectra of proteins via double quantum filtering. *Biochem Biophys Res Comm 117*:479–485.

Richards FM. 1977. Areas, volumes, packing and protein structure. *Annu Rev Biophys Bioeng 6*:151–176.

Richards FM, Lim WA. 1994. An analysis of packing in the protein folding problem. *Q Rev Biophys 26*:423–498.

Schneider DM, Dellwo MJ, Wand AJ. 1992. Fast internal main-chain dynamics of human ubiquitin. *Biochemistry 31*:3645–3652.

Stites WE, Gittis AG, Lattman EE, Shortle D. 1991. In a staphylococcal nuclease mutant the side-chain of a lysine replacing valine 66 is fully buried in the hydrophobic core. *J Mol Biol 221*:7–14.

Stone MJ, Chandrasekhar K, Holmgren A, Wright PE, Dyson HJ. 1993. Comparison of backbone and tryptophan side-chain dynamics of reduced and oxidized *Escherichia coli* thioredoxin using ^{15}N NMR relaxation measurements. *Biochemistry 32*:426–435.

Zhang O, Kay LE, Olivier JP, Forman-Kay JD. 1994. Backbone ^1H and ^{15}N resonance assignments of the N-terminal SH3 domain of drk in folded and unfolded states using enhanced-sensitivity pulsed field gradient NMR techniques. *J Biomol NMR 4*:845–858.